LANGLEY GRANT
IN-05-CR
320488
P.47

FINAL REPORT

Periodic Trim Solutions with hp-Version
Finite Elements in Time

NASA Grant NAG-1-1027

December 20, 1990

Prepared For:

Dr. Raymond G. Kvaternik
NASA Langley Research Center
M/S 340
Hampton, VA 23665

(NASA-CR-187705) PERIODIC TRIM SOLUTIONS WITH hp-VERSION FINITE ELEMENTS IN TIME Final Technical Report, 1 Jul. 1989 - 31 Dec. 1990 (Georgia Inst. of Tech.) 47 p CSCL 01C

N91-13449

Unclas
G3/05 0320488

Background

The purpose of this Grant is to investigate the possibilities of using hp-time finite elements to solve problems of rotorcraft trim and periodic response. Although conventional time-marching and Fourier methods have been somewhat successful, they do not always converge. Thus, methodologies need to be studied. The class of hp methods in time has the advantage that it is applicable even to unstable systems and easily converges on discontinuities in the solution.

Personnel

During the duration of this Grant, the Principal Investigator (Dr. David Peters) spend 0.9 man-months of effort; and Graduate Research Assistants Ay Su, Lin-Jin Hou, and Yi-Ren Wang spent 2.57, 1.00, and 0.75 man-months, respectively. The work of Mr. Su and Mr. Wang was primarily in providing flap-lag response for comparisons. Mr. Hou, however, did all of the finite-element coding.

Results

The results of this work include trimmed and untrimmed cases, flap and flap-lag cases, and are for both displacement and mixed formulations. The attached paper, to be presented at the AHS International Specialists' meeting on Rotorcraft Basic Research, summarizes the results. In addition, an oral presentation was given at the DAMUIBS workshop in September, 1990, at NASA Langley.

Periodic Trim Solutions with *hp*-Version Finite Elements in Time

Final Report
DAMVIBS Program
NASA Grant No. NAG-1-1027
12 December 1990

Professor David A. Peters
Graduate Research Assistant Lin-Jun Hou
School of Aerospace Engineering
Georgia Institute of Technology
Atlanta, Georgia 30332

Research Supported by
Army Aerostructures Laboratory
Langley Research Center

Periodic Trim Solutions with *hp*-Version Finite Elements in Time

Lin-Jun Hou[1] and David A. Peters[2]
School of Aerospace Engineering
Georgia Institute of Technology
Atlanta, GA 30332

December 12, 1990

ABSTRACT

We have studied finite elements in time as an alternative strategy for rotorcraft trim problems. The research treats linear flap and linearized flap-lag response both for quasi-trim and trim cases. The connection between Fourier series analysis and *hp*-finite elements for periodic problem is also examined. It is proved that Fourier series is a special case of space-time finite elements in which one element is used with a strong displacement formulation. Comparisons are made with respect to accuracy among Fourier analysis, displacement methods, and mixed methods over a variety parameters. The *hp* trade-off is studied for the periodic trim problem to provide an optimum step size and order of polynomial for a given error criteria. It is found that finite elements in time can outperform Fourier analysis for periodic problems, and for some given error criteria. The mixed method provides better results than does the displacement method.

[1]Graduate Research Assistant, School of Aerospace Engineering.
[2]Professor, School of Aerospace Engineering.

INTRODUCTION

Finite elements in the time domain have recently come into widespread use. Versions exist in a time-marching framework, in a Galerkin framework, in a Rayleigh-Ritz framework, and in a mixed formulation. Furthermore, recent *hp* work has demonstrated that the convergence of such methods is highly enhanced when one uses a weak formulation with test functions chosen so as to meet certain precise mathematical criteria on the continuity of the bilinear operator [13]. Thus far, these fast-converging *hp* methods have only been used on transient response (Floquent theory) [13] and on boundary-value problems (in optimal control) [14]. In this paper, we use this method on rotorcraft trim problems.

For hingeless rotorcraft dynamics, aeroelastic motions of the rotor blades and of the fuselage are coupled in forward flight thus makes the response problem fairly difficult. Analyses of pitch-flap and pitch-flap-lag dynamics in hover and flap dynamics in forward flight have been well documented [3] [6] [10], and rotorcraft trim is usually one of the most difficult aspects of the solution. In brief, to trim, one must find a periodic solution to a nonlinear, periodic-coefficient, differential equation subject to side constraints that certain force and moment balance equations must sum to zero. There are certain free (or trim) parameters in the problem that must be chosen so as to meet these side constraints, but it is not easy to find either the periodic solution or the unknown controls. Although conventional time-marching and Fourier methods have been somewhat successful, they do not always converge.

Hamilton's law of varying action has been applied to time finite elements [1] [2] [4]; recently, Borri *et al* [5] and Peters and Izadpanaph [13] provided a powerful alternative by using Hamilton's weak principle (HWP) to the numerical solution of ordinary differential equations in the time domain. Here, we apply Hamilton's weak principle for time finite elements to the problem of rotorcraft trim and periodic response. The work begins with the question of shape functions and compares the use of integrals of Legendre polynomials as shape functions to the use of Fourier series; since the latter enforce momentum periodicity (which is a natural boundary condition) they force a strong rather weak formulation. However, we need to firmly establish the connections between Fourier analysis and *hp*-finite elements for the periodic case.

Second, the trim constraints are treated as formal side constraints in the variational form of the problem. This turns out to be a benificial by-product of the *hp* methodology - namely that the unknown controls can augment the unknown coefficients in a formal way. In addition to the displacement method, the mixed method is also implemented in which displacement and momentum have seperate expansions. Finally, the inplane degrees of freedom is added. In terms of numerical issues, the *hp* trade-off is investigated; and the work herein will then show that how the *hp* trade-off is optimized for both methods, as advantages are verified for accuracy and efficiency.

- **Linear Flap**

For the linear flap problem, the equation of motion is derived for an idealized model of a hingeless rotor rigid blade. Aerodynamic forces are based on linear quasi-steady strip theory; small angle assumptions are made for induced angles and for the flap angle. The induced inflow is assumed to be uniform and is obtained from simple momentum theory. Also, the lift curve slope a, and blade chord c are assumed constant along the blade.

The equation of motion for flapping can then be obtained from moment equilibrium

$$\ddot{\beta} + C(\bar{t})\,\dot{\beta} + K(\bar{t})\,\beta = F(\bar{t}) \tag{1}$$

where

$$\begin{aligned}
C(\bar{t}) &= \frac{\gamma}{8}\,(1 + \frac{4}{3}\mu \sin \bar{t}) \\
K(\bar{t}) &= p^2 + \frac{\gamma}{8}(\frac{4}{3}\mu \cos \bar{t} + \mu^2 \sin 2\bar{t}) \\
F(\bar{t}) &= \frac{\gamma}{8}[(\theta_0 + \theta_s \sin \bar{t} + \theta_c \cos \bar{t})(1 + \frac{8}{3}\mu \sin \bar{t} + \mu^2 - \mu^2 \cos 2\bar{t}) \\
&- \lambda(\frac{4}{3} + 2\mu \sin \bar{t}) - \phi(1 + \frac{4}{3}\mu \sin \bar{t})] \\
\bar{t} &= \psi = \Omega t, \qquad \dot{(\;)} = \frac{d}{d\bar{t}}(\;)
\end{aligned}$$

FOURIER SERIES ANALYSIS

To implement a Fourier analysis, we express the flapping angle β in terms of a harmonic series with N_h harmonics and the number of terms $N = 2N_h + 1$

$$\begin{aligned}
\beta &= \sum_{i=1}^{N} \varphi_i(\bar{t}) q_i \\
&= q_1 + q_2 \cos \bar{t} + q_3 \sin \bar{t} + q_4 \cos 2\bar{t} + q_5 \sin 2\bar{t} + \ldots
\end{aligned}$$

We then apply Galerkin's scheme, multiply equation (1) by test functions φ_j, which are also harmonics, and integrate. We then have

$$\sum_{i=1}^{N} \int_0^{2\pi} (\ddot{\varphi}_i + C\dot{\varphi}_i + K\varphi_i)\, q_i \varphi_j d\bar{t} = \int_0^{2\pi} F\varphi_j \, d\bar{t} \quad j = 1, 2, \ldots, N \tag{2}$$

Integration by parts and use the periodicity of the φ_i yields

$$\sum_{i=1}^{N} \int_0^{2\pi} (\dot{\varphi}_i \dot{\varphi}_j - C\,\dot{\varphi}_i \varphi_j - K\,\varphi_i \varphi_j)\, q_i d\bar{t} = -\int_0^{2\pi} F\varphi_j \, d\bar{t} \tag{3}$$

Now, we consider for comparison the alternate approach of using finite elements in time by virture of Hamilton's strong principle

$$\delta \int_0^{2\pi} (T - V) d\bar{t} + \int_0^{2\pi} \delta W_{nc} d\bar{t} = 0 \tag{4}$$

where

$$T = \frac{1}{2}\dot{\beta}^2, \quad V = \frac{1}{2}K\beta^2, \quad \delta W_{nc} = (F - C\dot{\beta})\delta\beta$$

for the current problem. Substitution of the above into equation (4) yields

$$\int_0^{2\pi} (\dot{\beta}\delta\dot{\beta} - K\beta\delta\beta + F\beta - C\dot{\beta}\delta\beta) d\bar{t} = 0 \tag{5}$$

Let

$$\beta = \sum_{i=1}^{N} \varphi_i(\bar{t}) q_i \, , \quad \delta\beta = \sum_{j=1}^{N} \varphi_j(\bar{t}) \delta q_j$$

where the φ_i must be periodic, since equation (4) must be true for arbitrary δq_j. We will then obtain equation (3) as deriverd from Fourier series. The governing differential equation can also be recovered from equation (5) by integration by parts and use of the periodicity property on momentum. Thus, this proves that the Fourier series approach is a special case of finite elements in time in which harmonics are used as trial and shape functions for *one* element.

For the quasi-trim problem, the collective and cyclic pitch angles are given, $\theta = \theta_0 + \theta_c \cos \bar{t} + \theta_s \sin \bar{t}$, so as to suppress approximatly first harmonic cyclic flapping, $\beta_c, \beta_s \approx 0$, and thereby minimize rotor hub moments. For the trim problem, the trim parameters θ_0, θ_c, θ_s are treated as unknown controls to be found such that first harmonic flapping is identically zero.

The equations for these trim conditions, which can be taken as formal side constraints, are

$$\frac{1}{2\pi} \int_0^{2\pi} \beta d\bar{t} \;=\; \beta_0 \tag{6}$$

$$\frac{1}{\pi}\int_0^{2\pi} \beta \cos\bar{t}\; d\bar{t} \;=\; 0 \tag{7}$$
$$\frac{1}{\pi}\int_0^{2\pi} \beta \sin\bar{t}\; d\bar{t} \;=\; 0 \tag{8}$$

Due to the orthogonality of triogonometric function, equations (7), (8) yield for Fourier analysis

$$q_2 \;=\; 0\;, \qquad q_3 \;=\; 0$$

Equation (6) can also be replaced by an alternative form in which thrust is specified

$$\frac{1}{2\pi}\int_0^{2\pi} C_T(\bar{t})\; d\bar{t} = C_{T0}$$

where $C_T(\bar{t})$ is obtained by blade element theory

$$C_T(\bar{t}) = \int_0^1 \frac{abc}{2\pi R}[(x+\mu\sin\bar{t})^2\theta \;-\; (x+\mu\sin\bar{t})(\lambda + x\dot{\beta} + \mu\beta\cos\bar{t})]dx$$

For the trim condition, the minimum order necessary for the Fourier series approach is first harmonic cyclic flapping (q_1, q_2, q_3); since with use of q_1 only as a one-term approximation (i.e., $\beta = \beta_0$), equations (7) (8) will be identically zero which results in a singular matrix. Physically, three polynomials are required for Fourier series ($N_h = 1$) because of three trim constraints; and the periodicity conditions are automatically satisfied. Similar requirement on the number of polynomials in trim problem occurs in the displacement and mixed methods, as will be discussed later. Table 1 summaries the number of harmonics and required number of polynomials for the trim case. It is noteworthy that the unknown trim parameters θ_0, θ_c and θ_s are included in the aerodynamic force term $F(\bar{t})$ and should be moved to the left hand side in the matrix formulation for solution.

DISPLACEMENT METHOD

For the displacement formulation, we start with Hamilton's law of varying action

$$\int_{t_i}^{t_f} (\delta L + \delta q^T Q_{nc})dt - \sum_{i=1}^{n} \frac{\partial L}{\partial \dot{q}_i} \delta q_i \mid_{t_i}^{t_f} = 0 \tag{9}$$

With a weak constraint of momentum [19], the Hamilton's weak principle (primal or displacement form) is then

$$\delta \int_{t_i}^{t_f} L \, dt + \int_{t_i}^{t_f} \delta W_{nc} \, dt - \sum_{i=1}^{n} \delta q_i \cdot p_i \mid_{t_i}^{t_f} = 0 \tag{10}$$

where the trailing term $-\sum_{i=1}^{n} \delta q_i \cdot p_i$ can be thought of as the virtual action δA entering (or leaving) the time boundaries t_i and t_f. Thus, one might interprete equation (10) as a variational statement of elasto-dynamics, "the variation of the action plus the virtual action over the time interval $t_i < 0 < t_f$ plus the net virtual action across the time boundaries must sum to zero".

Before proceeding further in displacement development, we integrate equation (10) by parts for the linear flapping problem which yields

$$\int_0^{2\pi} (\ddot{\beta} + C\dot{\beta} + K\beta - F)\delta\beta d\bar{t} - (p - \dot{\beta})\delta\beta \mid_0^{2\pi} = 0 \tag{11}$$

Obviously, for equation (11) to be valid for all $\delta\beta(\bar{t})$, the following equations must hold.

$$\ddot{\beta} + C\dot{\beta} + K\beta = F \tag{12}$$

$$p_0 = \dot{\beta}(0) \tag{13}$$

$$p_T = \dot{\beta}(T) \tag{14}$$

The above relations imply that the governing differential equation and boundary conditions for momenta are satisfied by equation (10). Even for a conservative system, initial value problems are not-self-adjoint and thus they do not yield the minimum of a functional in the classical sense. However, the variational statement is valid. One can think of Eq. (10) as the time integral of the virtual work where the virtual displacements at the boundary times (δq_i at t_i and t_f) may or may not be set to zero.

As shown in Ref. [16], certain geometric boundary conditions must be satisfied for the admissable set of trial and test functions to have a stable numerical formulation. For the trial functions, geometric boundary condition on $\beta(0)$ or $\beta(T)$, must be exactly satisfied. For the test functions $\delta\beta(0)$ or $\delta\beta(T)$ must be zero if either p_0 or p_T is unknown, respectively.

Eq. (11) can also be interpreted as the sum of the Galerkin weighted residuals set equal to zero. For an approximate solution $\tilde{\beta}$, it can also be interpreted as an error functional $E(\tilde{\beta}, \delta\tilde{\beta})$. From the concepts of finite elements, one can set $E = 0$ for some limited class of $\delta\tilde{\beta}$. However, the error functional is not bilinear if either p_0 or p_T is unknown. It follows that if either p_0 or p_T is unknown, $\delta\tilde{\beta}(0)$ or $\delta\tilde{\beta}(T)$ must be set to zero to eliminate the unknowns from the trailing terms. Thus, for boundary value problems, if $\beta(0)$ and p_T are prescribed (p_0 unknown) then we set $\delta\tilde{\beta}(0) = 0$. On the other hand, for initial value problems, if $\beta(0)$ and p_0 are known but p_T unknown, then we set $\delta\tilde{\beta}(T) = 0$ but $\delta\tilde{\beta}(0) \neq 0$. If $\delta\tilde{\beta}(0) \neq 0$, then setting $E(\tilde{\beta}, \delta\tilde{\beta}) = 0$ ensures that $p_0 \rightarrow \dot{\beta}(0)$ which provides weak convergence to the natural boundary condition. Similar arguments holds for other combinations of end conditions.

For the periodic problem, $\beta(0) = \beta(T)$ is a strong condition whereas $\dot{\beta}(0) = \dot{\beta}(T)$ is a weak condition enforced through $p_0 = p_T$ which can be thought of as a Lagrange multiplier. Equation (10) can then be written as

$$\int_0^{2\pi}(\dot{\beta}\delta\beta - C\dot{\beta}\delta\beta - K\beta\delta\beta + F\delta\beta)d\bar{t} - \lambda_p[\delta\beta(2\pi) - \delta\beta(0)] = 0 \qquad (15)$$

Since λ_p is unknown, we must set $\delta\beta(2\pi) = \delta\beta(0)$ for a bilinear formulation. For numerical solution, we choose the integrals of Legendre polynomials $P_j(x)$ as shape functions for β and $\delta\beta$

$$\beta = \sum_{j=1}^{N} \Phi_j(\eta)q_j\,, \qquad \delta\beta = \sum_{i=1}^{N} \Phi_i(\eta)\delta q_i \qquad (16)$$

where N is the number of terms in β or $\delta\beta$ and

$$\begin{aligned} \Phi_1 &= \frac{1-\eta}{2}, \quad \Phi_2 = \frac{1+\eta}{2} \qquad (-1 \le \eta \le 1) \\ \Phi_{j+1} &= \sqrt{\frac{2j-1}{2}} \int_{-1}^{\eta} P_{j-1}(x)dx \qquad j = 2, 3, \ldots, N-1 \end{aligned}$$

If the Lagrange multiplier is retained as an unknown (not bilinear), then there is no constraint on $\delta\beta$ and we have $N+1$ equations in $N+1$ unknowns. (Recall that the $(N+1)^{st}$ equation is the required constraint $\beta(0) = \beta(2\pi)$.) However, if $\delta\beta$ is constrained, one equation is lost and λ_p is eliminated yielding N equations in N unknowns.

- *Momentum in the Displacement Method*

Momentum in the displacement method can be obtained in three ways :

(i) *Derivatives of displacements (or rotations)*

$$P(\bar{t}_1) = \dot{\beta}(\eta) = \sum_{j=1}^{N} \Phi_j' \frac{1}{\pi} q_j \qquad (17)$$

where $\dot{(\,)} = \frac{d()}{dt} = \frac{1}{\pi}\frac{d()}{d\eta} = \frac{1}{\pi}(\,)'$, and $\eta = \frac{\bar{t}_1}{\pi} - 1$.

(ii) *Using Lagrange multiplier with derivatives of displacements involved in integral formulation*

$$P(\bar{t}_1) = \lambda_P + \int_0^{\bar{t}_1} (F - C\dot{\beta} - K\beta) d\bar{t} \tag{18}$$

(iii) *Using Lagrange multiplier without derivatives of displacements involved in integral formulation*

Integration of equation (18) by parts yields

$$P(\bar{t}_1) = \lambda_P - C\beta \,|_0^{\bar{t}_1} + \int_0^{\bar{t}_1} (F + \dot{C}\beta - K\beta) d\bar{t} \tag{19}$$

The reason that equation (17) is not advisable, is that there is sensitivity problem in convergence of derivatives of shape functions, Φ_j', which may occur in (i). By virture of the Lagrange multiplier, strategy (ii) (which was used in Ref. [13]) improves the accuracy; and strategy (iii), applied in this work, gives the best results. As the number of elements and order of polynomials increased, (ii) and (iii) approach the same results rapidly.

With multiple elements M having $(N-1)^{th}$ order polynomials, the flapping angle β is continuous between elements. This requires $M-1$ constraint equations, and the periodicity provides one more. This is balanced either by M unknowns (which are the momenta at nodes) or by the M constraints on $\delta\beta$ required to eliminate those momenta. These nodal momenta can be extracted by discretization of the trailing terms of the displacement formulation (15).

$$\begin{aligned} Trailing\ terms \ &= \ \lambda_M[\delta\beta^{(1)}(0) - \delta\beta^{(M)}(2\pi)] \\ &+ \ \sum_{m=1}^{M-1} \lambda_m[\delta\beta^{(m+1)}(\bar{t}_{m+1}) - \delta\beta^{(m)}(\bar{t}_{m+1})] \end{aligned} \tag{20}$$

Thus, the λ_m can be retained or the $\delta\beta$ be restricted. The trim constraint equations for multi-elements with $(N-1)^{th}$ order polynomial are

$$\sum_{m=1}^{M} \int_{-1}^{1} \sum_{j=1}^{N} q_j^{(m)} \Phi_j \cos\bar{t} \ d\eta \ = \ 0$$

$$\sum_{m=1}^{M} \int_{-1}^{1} \sum_{j=1}^{N} q_j^{(m)} \Phi_j \, \sin \bar{t} \, d\eta = 0 \tag{21}$$

$$\sum_{m=1}^{M} \sum_{j=2}^{N} \bar{q}_j^{(m)} \int_{-1}^{1} [(\frac{1}{3} + \frac{\mu}{2} \sin \bar{t}) \Phi_j' + \frac{\pi}{2M} \mu^2 \sin 2\bar{t} \, \Phi_j] \, d\eta$$
$$- \frac{2\pi}{3} \theta_0 (1 + \frac{3}{2} \mu^2) - \mu \pi \theta_s = \frac{-4C_{T0}}{a\sigma} \pi - \lambda \pi$$

where

$$\begin{aligned} \bar{t} &= \bar{t}_m + \frac{1+\eta}{2} \triangle \bar{t} \\ &= \frac{2\pi}{M}(m-1) + \frac{1+\eta}{2} \frac{2\pi}{M} \quad (-1 \leq \eta \leq 1) \end{aligned}$$

Numerical difficulties arise in trim problems if too few terms are taken. With a one element model, the number of polynomials has to be at least four since we have three trim constraints and one periodicity constraint. With multiple element modeling, additional periodicity constraints are required between elements, thus the need is for more than four polynomials. The relations between number of polynomials and required number of elements are shown in Table 2.

MIXED METHOD

The momenta, like displacements, are treated as additional field variables in the mixed method. The mixed formulation derived from Hamilton's weak principle [5] is

$$\int_{t_i}^{t_f} (\delta \dot{q}^T \, p \; - \; \delta \dot{p}^T \, q \; - \; \delta H \; + \; \delta q^T \, Q) dt = (\delta q^T \, p \; - \; \delta p^T \, q) \, |_{t_i}^{t_f} \tag{22}$$

where q denotes the set of generalized coordinates, Q the set of nonconservative generalized forces applied to the system, $L(q, \dot{q}, t)$ the Lagrangian of the system, $p = \partial L/\partial \dot{q}$ the set of generalized momenta, and $H = p^T\dot{q} - L$ the Hamiltonian.

For the flapping problem,

$$\begin{aligned} L &= \frac{1}{2}\dot{\beta}^2 - \frac{1}{2}K\,\beta^2 \\ Q &= F - C\dot{\beta} \\ H &= \frac{1}{2}\dot{\beta}^2 + \frac{1}{2}K\,\beta^2 \\ p &= \dot{\beta} \end{aligned}$$

The mixed formulation for the flapping problem is then

$$\begin{aligned} \int_0^{2\pi} (\delta\dot{\beta}\,p &- \delta\dot{p}\,\beta - p\,\delta p - K\beta\,\delta\beta + F\,\delta\beta - C\,p\,\delta\beta)\,d\bar{t} \\ &= (\delta\beta\,p - \delta p\,\beta)\,\big|_0^{2\pi} \end{aligned} \tag{23}$$

where the variations of β and p are independent, and all boundary conditions are of the natural (or weak) type. Since the derivatives exist only in virtual displacements $\delta\beta$ and virtual momentum δp, it is then possible to implement C^0 continuous shape functions for the test functions and discontinuous functions for the trial functions.

The C^0 shape functions are chosen to be hierarchical "bubble" functions

$$\begin{aligned} \delta p &= \delta p_1(1-\tau) + \delta p_2\tau + (1-\tau)\tau\sum_{i=1}^{N-2}\delta p_i^* B_i(\tau) f_i, \quad (0 \le \tau \le 1) \\ \delta\beta &= \delta q_1(1-\tau) + \delta q_2\tau + (1-\tau)\tau\sum_{i=1}^{N-2}\delta q_i^* B_i(\tau) f_i, \quad (0 \le \tau \le 1) \end{aligned} \tag{24}$$

where $B_i(\tau) = G_{i-1}(P, Q; \tau)$ are Jacobi polynomials. P, Q are parameters and f_i the normalizing factor; and N is the number of terms in δp or $\delta\beta$.

The approximate values of p and β are taken as continuous function within the element while allowing for distinct, discrete values on the boundaries of elements [15].

$$
\begin{aligned}
p &= \sum_{j=1}^{N-1} \bar{p}_j \alpha_j(\tau), \;\; \beta = \sum_{j=1}^{N-1} \bar{q}_j \alpha_j(\tau) \qquad (0 < \tau < 1) \\
p &= \hat{p}_1, \;\; \beta = \hat{\beta}_1, \qquad (\tau = 0) \\
p &= \hat{p}_2, \;\; \beta = \hat{\beta}_2, \qquad (\tau = 1)
\end{aligned} \tag{25}
$$

Note that there are $N-1$ $\bar{p}$ terms and one unknown $\hat{p}$ giving N unknown p (or β) terms. The $\delta\beta$ and δp are assumed as free variations which exist even when p and β are prescribed. Hodges and Hou [9] showed the derivation of shape functions $\alpha_j(\tau)$ and normalizing factors f_i for mixed p-version finite element.

Unlike in the displacement method, the trial functions β, p are discontinuous between elements in the mixed method, while the test functions $\delta\beta$, δp are continuous between elements including the periodic connection. The reason is to be found below.

First, we rewrite the trailing terms of the mixed formulation (21) for a one-element model

$$
(\delta\beta\, p - \delta p\, \beta)\,|_0^{2\pi} = \lambda_p[\delta\beta(2\pi) - \delta\beta(0)] - \lambda_\beta[\delta p(2\pi) - \delta p(0)] \tag{26}
$$

where

$$
\hat{p}_1 = \hat{p}_2 \equiv \lambda_p, \quad \hat{\beta}_1 = \hat{\beta}_2 \equiv \lambda_\beta
$$

Obviously, the continuity of $\delta\beta$ and δp is required to eliminate the unknowns λ_p, λ_β at end of the period.

For hp finite elements, the nodal momenta can be recovered by following the same steps as equation (20) and by discretizing the time domain in trailing terms

$$Trailing\,term = \lambda_p^{(M)}[\delta\beta^{(M)}(2\pi) - \delta\beta^{(1)}(0)] + \sum_{m=1}^{M-1} \lambda_p^{(m)}[\delta\beta^{(m)}(\bar{t}_{m+1}) - \delta\beta^{(m+1)}(\bar{t}_{m+1})]$$

$$- \lambda_\beta^{(M)}[\delta p^{(M)}(2\pi) - \delta p^{(1)}(0)] - \sum_{m=1}^{M-1} \lambda_\beta^{(m)}[\delta p^{(m)}(\bar{t}_{m+1}) - \delta p^{(m+1)}(\bar{t}_{m+1})] \quad (27)$$

Thus, the nodal values $\lambda_p^{(m)}$, $\lambda_\beta^{(m)}$ can then be found by solving equations associated with independent coefficients $\delta q_i^{(m)}$, $\delta p_i^{(m)}$ $(i = 1, 2, \ldots, N-1)$.

The trim equations for the mixed method are

$$\sum_{m=1}^{M} \left[\sum_{j=1}^{N-1} \bar{q}_j^{(m)} \int_0^1 \alpha_j \cdot \cos\bar{t}\ \ d\tau \right] = 0$$

$$\sum_{m=1}^{M} \left[\sum_{j=1}^{N-1} \bar{q}_j^{(m)} \int_0^1 \alpha_j \cdot \sin\bar{t}\ \ d\tau \right] = 0 \quad (28)$$

$$\sum_{m=1}^{M} \left[\sum_{j=1}^{N-1} \bar{q}_j^{(m)} \frac{\pi}{M}\mu^2 \int_0^1 \sin 2\bar{t}\ \alpha_j\ d\tau + \sum_{j=1}^{N-1} \bar{p}_j^{(m)} \frac{2\pi}{M} \int_0^1 (\frac{1}{3} + \frac{\mu}{2}\sin\bar{t})\alpha_j d\tau \right]$$

$$-\frac{2\pi}{3}\theta_0(1 + \frac{3}{2}\mu^2) - \mu\pi\theta_s = \frac{-4C_{T0}}{a\sigma}\pi - \lambda\pi$$

where

$$\begin{aligned} \bar{t} &= \bar{t}_m + \tau\Delta\bar{t} \\ &= \frac{2\pi}{M}(m-1) + \tau\frac{2\pi}{M} \qquad (0 \le \tau \le 1) \end{aligned}$$

Again, there is a minimum requirement for the number of polynomials in the mixed method trim problem. With Lagrange multiplier, the periodicity constraints on generalized coordinates are enforced "implicitly"; thus, the minimum polynomial number for trim is six for any number of elements since there are two generalized coordinates, displacement and momentum. This relation is depicted in Table 3.

- **Flap-Lag**

We use the same model as in Ref. [8] for the flap-lag problem. The schematical model is shown in Fig. 1. It consists of a centrally hinged rigid blade, with flap and lag restraint springs to simulate the elastic coupling characteristics of the actual blade. The spring stiffnesses are chosen so that the uncoupled, rotating flap and lag natural frequencies coincide with the corresponding first mode rotating natural frequencies of the elastic blade. The effects of induced flow, blade equilibrium, and aerodynamic stiffness on aerodynamic terms are retained. We further assume that the drag coefficient C_{d0} is small with respect to the lift curve slope, and reversed flow is neglected.

The nonlinear equations of motion of this model are [7]

$$\begin{aligned} \ddot{\beta} + \sin\beta\cos\beta(1+\dot{\zeta})^2 + (P-1)(\beta-\beta_{pc}) + Z\zeta &= \int_0^1 \bar{F}_\beta \bar{r}\, d\bar{r} \qquad (29) \\ \cos^2\beta\,\ddot{\zeta} - 2\sin\beta\cos\beta(1+\dot{\zeta})\dot{\beta} + W\zeta + Z(\beta-\beta_{pc}) &= \cos\beta\int_0^1 \bar{F}_\zeta \bar{r}\, d\bar{r} \end{aligned}$$

where $\bar{F}_\beta$ and $\bar{F}_\zeta$ are the nondimensional airloads perpendicular to the blade and respectively in the flap and lead directions. The elastic terms approximated by small β, ζ formulas [12] and small pitch angle assumption are

$$P = 1 + \omega_\beta^2 = p^2, \quad W = \omega_\zeta^2, \quad Z = R(\omega_\zeta^2 - \omega_\beta^2)\theta \qquad (30)$$

For the linearized model, we make small perturbations about a periodic equilibrium motion of the nonlinear system. Denoting $\bar{\theta}(\bar{t})$, $\bar{\zeta}(\bar{t})$ and $\bar{\beta}(\bar{t})$ as the equilibrium values of θ, ζ and β and one can write the perturbation expansions :

$$\zeta = \bar{\zeta} + \delta\zeta, \quad \beta = \bar{\beta} + \delta\beta, \quad \theta = \bar{\theta} + \theta_\beta\delta\beta + \theta_\zeta\delta\zeta \qquad (31)$$

where

$$\bar{\theta} = \theta_0 + \theta_s \sin\bar{t} + \theta_c\cos\bar{t} + \theta_\beta(\bar{\beta} - \beta_{pc}) + \theta_\zeta\bar{\zeta}$$

and θ_β and θ_ζ are pitch-flap and pitch-lag coupling parameters. Positive θ_β or θ_ζ implies that the blade pitches up due to positive flapping or lead inplane motions.

Substituting Eq.(31) into the nonlinear equations (29), cancelling the appropriate equilibrium terms and neglecting the higher order quantities $\bar{\zeta}$, $\dot{\bar{\zeta}}$, $\bar{\beta}^2$, $\beta\dot{\bar{\beta}}$, and $\dot{\bar{\beta}}^2$ with respect to unity; we obtain the linearized equation for flap-lag forced response :

$$\left\{ \begin{array}{c} \delta\ddot{\beta} \\ \delta\ddot{\zeta} \end{array} \right\} + [C(\bar{t})] \left\{ \begin{array}{c} \delta\dot{\beta} \\ \delta\dot{\zeta} \end{array} \right\} + [K(\bar{t})] \left\{ \begin{array}{c} \delta\beta \\ \delta\zeta \end{array} \right\} =$$

$$[L(\bar{t})] \left\{ \begin{array}{c} \dot{\bar{\beta}} \\ \bar{\beta} \end{array} \right\} + [M(\bar{t})] \left\{ \begin{array}{c} \bar{\theta} \\ \bar{\phi} \end{array} \right\} + [N(\bar{t})] \left\{ \begin{array}{c} \bar{\bar{\beta}} \\ C_{d0}/a \end{array} \right\} + \{O(\bar{t})\}\, \beta_{pc} \tag{32}$$

where

$$[C(\bar{t})] = \left[\begin{array}{cc} \frac{\gamma}{8}(1 + \frac{4}{3}\mu s\bar{t}) & \begin{array}{c} \frac{\gamma}{8}(\bar{\phi} + \frac{4}{3}\mu c\bar{t}\bar{\beta} + \dot{\bar{\beta}}) \\ -2\frac{\gamma}{8}\bar{\theta}(1 + \frac{4}{3}\mu s\bar{t}) + 2\bar{\beta} \end{array} \\ & \\ \begin{array}{c} -2\frac{\gamma}{8}(\bar{\phi} + \frac{4}{3}\mu c\bar{t}\bar{\beta} + \dot{\bar{\beta}}) \\ +\frac{\gamma}{8}\bar{\theta}(1 + \frac{4}{3}\mu s\bar{t}) - 2\bar{\beta} \end{array} & \begin{array}{c} \frac{\gamma}{8}\bar{\theta}(\bar{\phi} + \frac{4}{3}\mu c\bar{t}\bar{\beta} + \dot{\bar{\beta}}) - 2\bar{\beta}\dot{\bar{\beta}} \\ +2\frac{C_{d0}}{a}\frac{\gamma}{8}(1 + \frac{4}{3}\mu s\bar{t}) \end{array} \end{array} \right] \tag{33}$$

$$
[K(\bar{t})] = \begin{bmatrix}
\begin{array}{c} P \\ +\frac{\gamma}{8}(\frac{4}{3}\mu c\bar{t} + 2\mu^2 s\bar{t}c\bar{t}) \\ -\frac{\gamma}{8}\theta_\beta(1 + \frac{8}{3}\mu s\bar{t} + 2\mu^2 s^2\bar{t}) \end{array} &
\begin{array}{c} Z + \frac{\gamma}{8}\mu c\bar{t}(\frac{3}{2}\bar{\phi} + \frac{4}{3}\dot{\bar{\beta}}) \\ -2\frac{\gamma}{8}\bar{\theta}(\frac{4}{3}\mu c\bar{t} + 2\mu^2 s\bar{t}c\bar{t}) \\ +2\frac{\gamma}{8}\bar{\beta}(\mu^2 c^2\bar{t} - \mu^2 s^2\bar{t} - \frac{2}{3}\mu s\bar{t}) \\ -\frac{\gamma}{8}\theta_\zeta(1 + \frac{8}{3}\mu s\bar{t} + 2\mu^2 s^2\bar{t}) \end{array} \\
\\
\begin{array}{c} Z - 2\dot{\bar{\beta}} - 2\frac{\gamma}{8}\mu c\bar{t}(\frac{2}{3}\phi + \frac{4}{3}\dot{\bar{\beta}}) \\ \\ +\frac{\gamma}{8}\bar{\theta}(\frac{4}{3}\mu c\bar{t} + 2\mu^2 s\bar{t}c\bar{t}) \\ \\ -4\frac{\gamma}{8}\bar{\beta}\mu^2 c^2\bar{t} + R\theta_\beta(\bar{\beta} - \beta_{pc}) \\ \cdot(\omega_\zeta^2 - \omega_\beta^2) \\ +\frac{\gamma}{8}\theta_\beta[\bar{\phi}(1 + \frac{3}{2}\mu s\bar{t}) + \dot{\bar{\beta}}(1 + \frac{4}{3}\mu s\bar{t}) \\ \\ +\bar{\beta}(\frac{4}{3}\mu c\bar{t} + 2\mu^2 s\bar{t}c\bar{t})] \end{array} &
\begin{array}{c} W + \frac{\gamma}{8}[2\frac{C_{d0}}{a}(\frac{4}{3}\mu c\bar{t} + 2\mu^2 s\bar{t}c\bar{t}) \\ +\mu c\bar{t}\bar{\theta} \\ \cdot(\frac{3}{2}\bar{\phi} + \frac{4}{3}\dot{\bar{\beta}}) - \bar{\beta}\bar{\theta}(\frac{4}{3}\mu s\bar{t} + 2\mu^2 s^2\bar{t} \\ -2\mu^2 c^2\bar{t}) \\ +2\mu s\bar{t}\bar{\beta}(\frac{3}{2}\bar{\phi} + \frac{4}{3}\dot{\bar{\beta}} + 2\mu c\bar{t}\bar{\beta})] \\ +\frac{\gamma}{8}\theta_\zeta[\bar{\phi}(1 + \frac{3}{2}\mu s\bar{t}) \\ +\bar{\beta}(\frac{4}{3}\mu c\bar{t} + 2\mu^2 s\bar{t}c\bar{t}) \\ +\dot{\bar{\beta}}(1 + \frac{4}{3}\mu s\bar{t})] \end{array}
\end{bmatrix} \tag{34}
$$

$$[L(\bar{t})] = \begin{bmatrix} -\frac{\gamma}{8}(1+\frac{4}{3}s\bar{t}) & -P-\frac{\gamma}{8}(\frac{4}{3}\mu c\bar{t}+2\mu^2 s\bar{t}c\bar{t}) \\ \frac{\gamma}{8}(2\bar{\phi}+\frac{8}{3}\bar{\beta}\mu c\bar{t}+\dot{\bar{\beta}}) & \frac{\gamma}{8}(3\bar{\phi}\mu c\bar{t}+2\mu^2 c^2\bar{t}\bar{\beta}) \\ -\frac{\gamma}{8}\bar{\theta}(1+\frac{4}{3}\mu s\bar{t})+2\bar{\beta} & -\frac{\gamma}{8}\bar{\theta}(\frac{4}{3}\mu c\bar{t}+2\mu^2 c\bar{t}s\bar{t}) \\ & -Z-R(\omega_\zeta^2-\omega_\beta^2)\theta_\beta \end{bmatrix} \tag{35}$$

$$[M(\bar{t})] = \begin{bmatrix} \frac{\gamma}{8}(1+\frac{8}{3}\mu s\bar{t}+2\mu^2 s^2\bar{t}) & -\frac{\gamma}{8}(1+\frac{3}{2}\mu s\bar{t}) \\ -\frac{\gamma}{8}\bar{\phi}(1+\frac{3}{2}\mu s\bar{t}) & \frac{\gamma}{8}(\frac{9}{8}\bar{\phi}) \end{bmatrix} \tag{36}$$

$$[N(\bar{t})] = \begin{bmatrix} -1 & 0 \\ 0 & -\frac{\gamma}{8}(1+\frac{8}{3}\mu s\bar{t}+2\mu^2 s^2\bar{t}) \end{bmatrix} \tag{37}$$

$$\{O(\bar{t})\} = \begin{Bmatrix} P-1 \\ Z+R(\omega_\zeta^2-\omega_\beta^2)\theta_\beta \end{Bmatrix} \tag{38}$$

Due to the nonlinear effects of flap-lag coupling for trimmed flight with constant C_T, iterations for the solutions are required. To speed up the convergence, formulas for θ_0, θ_s and θ_c in Ref. [11] by harmonic balance can be used as the first guess.

ERROR ANALYSIS

The shape functions are integrals of Legendre polynomials, $\Phi(\eta)$ for the displacement method; and are Jacobi polynomials $B_j(\tau)$ for the mixed method. These polynomials can be related as follows

$$\Phi_j = C_j\,(\eta^2-1)\,B_{j-1}, \quad j \geq 2 \quad (-1 \leq \eta \leq 1) \tag{39}$$

where $\tau = \frac{\eta+1}{2}$ and C_j is constant.

In order to express the characteristics of shape functions; errors are measured at the zeros (roots) of shape functions. The roots of integral of Legendre polynomials, for example, are more closely grouped near the endpoints.

This indicates that the polynomials are able to oscillate with increased frequency near the endpoints, and are better suited for approximating singular behavior which occurs at the endpoints than are trigonometric functions or uniform h-version meshes. For trigonometric functions, the roots are evenly distributed in the interval $-1 \leq x \leq 1$ and they have the important property that they "absorb" singularties at the finite element boundaries. Equation (39) also indicates that the zeros of Jacobi polynomials and the integrals of Legendre polynomials are equivalent. Table 4 and 5 show the number of zeros and polynoimial order in the mixed and displacement formulations.

The shape functions in the displacement method start with linear functions ($N = 2$), since the order of the polynomial $n = N - 1$. We thus need 2 points in each element for error analysis, which would be the nodes of elements. For $N = 3$, the quadratic polynomial needs an additional point to measure error which is the zero of next higher order polynomial. By keeping the state variables in their primative forms, the mixed method is able to start with constant ($N = 2$ in Eq. (25)) for its shape function since the order of polynomial $n = N - 2$. Following the same argument as in the displacement method, the measured points for N^{th} polynomial are the zeros of $(N+1)^{th}$ order polynomial.

Denoted by E_d, E_m, the norm error for displacement and mixed methods are defined seperatly as

$$E_d = \sqrt{\frac{\sum_{m=1}^{M}\left\{(\Delta\hat{\beta}^{(m)})^2 + \sum_{j=2}^{N-1}(\Delta\beta_j^{(m)})^2 + [(\Delta\hat{p}^{(m)})^2 + \sum_{j=2}^{N-1}(\Delta p_j^{(m)})^2]\cdot(W)^2\right\}}{\sum_{m=1}^{M}\left\{(\hat{\beta}_{ex}^{(m)})^2 + \sum_{j=2}^{N-1}(\beta_{jex}^{(m)})^2 + [(\hat{p}_{ex}^{(m)})^2 + \sum_{j=2}^{N-1}(p_{jex}^{(m)})^2]\cdot(W)^2\right\}}}$$

$$E_m = \sqrt{\frac{\sum_{m=1}^{M}\left\{(\Delta\hat{\beta}^{(m)})^2 + \sum_{j=2}^{N}(\Delta\beta_j^{(m)})^2 + [(\Delta\hat{p}^{(m)})^2 + \sum_{j=2}^{N}(\Delta p_j^{(m)})^2]\cdot(W)^2\right\}}{\sum_{m=1}^{M}\left\{(\hat{\beta}_{ex}^{(m)})^2 + \sum_{j=2}^{N}(\beta_{jex}^{(m)})^2 + [(\hat{p}_{ex}^{(m)})^2 + \sum_{j=2}^{N}(p_{jex}^{(m)})^2]\cdot(W)^2\right\}}}$$

where weight $W = T/2\pi$; $\Delta\hat{\beta}^{(m)}$ is the error at node of m^{th} element, and $\Delta\beta_j^{(m)}$ is the error at j^{th} zero within element.

For linear flap quasi-trim, trim and linearized flap-lag quasi-trim problems, essentially exact solutions can be obtained by Fourier series analysis. Since the Fourier series approach is a special case of time finite elements using one element, Figures 2, 3 and 4 illustrate the convergence behaviors of three approaches for quasi-trim and trim cases by single element modeling. Fourier analysis obviously gives excellent accuracy with respect to the number of floating point operations and CPU. Realizing that even the mixed formulation has almost twice the number of unknowns as in the displacement formulation and the Fourier analysis, and thus increase the number of operations and the size of the matrix; it yields a very sparse matrix which would be significantly influence the computation efficiency as will be shown later.

With multi-elements modeling, Fig. 5 (in which number of elements progresses as 1,2,4,8,16 and 32) compares the number of floating-point operations (see formulation in Ref. [13]) between the displacement method and the Fourier analysis. It shows that the displacement method is not competitive with classical Fourier analysis. Figures 6 through 9 compare the norm error with regard to the number of degrees of freedom for quasi-trim and trim cases. Without consideration of computational efficiency, the Fourier approach always gives the best results. However, the main objective here is to obtain satisfying accuracy with highest efficiency (or minimum CPU). In Figures 10-13, norm errors are plotted against CPU (on UNIX Sequent S81 computer) for the linear flap problem; and Figures 14 - 17 are for linearized flap-lag problem. Figures 10, 11 show that the mixed method is very competitive with the Fourier approach and is faster than the displacement method for a specified error requirement for the quasi-trim case. The advantage of mixed formulation in computation efficiency becomes obvious for the trim case as shown in Figures 12, 13. It is shown that at any given error criteria or CPU, the mixed method provides an optimum choice of number of elements and polynomial order (i.e., *hp* trade-off) due to the advantage of matrix sparsity.

In general, 4 linear elements in the mixed method is appopriate for moderate error criteria (1%), and 4 to 8 higher order elements for more stringent error criteria. However, the *hp* trade-off is not obvious in the displacement method, and the family of curves tends to converge with a slope of -5 to -6. More precisely, the relation between the norm error and CPU in the displacement method can be formulated as following

$$\frac{E_2}{E_1} \simeq \left(\frac{CPU_1}{CPU_2}\right)^{5\sim6} \tag{40}$$

In another words, for a factor of 10 improvement in accuracy, displacement method needs 1.5 times the CPU; and a factor of 100 improvement needs 2.5 times the CPU. Comparing both methods for the flap-lag problem in Figures 14 - 17, we can see clearly that mixed method is much faster than the displacement method for any given error criteria. Furthermore, the sparsity of matrix for mixed method has not yet been fully utilized, which will increase the advantage of the mixed method.

CONCLUSIONS

Finite elements in time (FET) are applied on rotorcraft trim problems in which Fourier series analysis, displacement and mixed methods are implemented and verified for accuracy and efficiency. Examples include linear flap and linearized flap-lag problems. It is proved that Fourier series can be thought of as a special case of finite elements in time, and the results also show that the mixed method in FET can outperform conventional Fourier analysis for rotor trim problems. The shape functions for different methods are chosen according to the characteristics of associated formulations. Thus, the integrals of Legendre polynomials are preferrable for the displacement method while Jacobi ploynomials are preferrable for the mixed method.

The mixed method shows the advantage of efficiency at a given accuracy. From *hp* trade-off analysis, it seems that 4 to 8 elements in the mixed method provide best results for any order polynomial for any given error criteria, while the *hp* trade-off is not sensitive in the displacement method, for which all the curves have similar convergence behavior.

Acknowledgement

This work was sponsored by the Army Aerostructures Lab, Langley Research Center, under the DAMVIBS program, NASA Grant No. NAG-1-1027; Dr. Ray Kvaternik, Technical Monitor.

Table 1. No. of Polynomials for Trim Using Fourier Series

Fourier Series			
No. of Harmonics N_h	β	No. of Poly $= 2N_h + 1$	Req. Poly No.
0	—	1*	3
1		3	3
2		5	3
* *singular matrix*			

Table 2. No. of Polynomials for Trim Using Displacement Method

Displacement Method				
M	N	β	No. of Poly $= MN$	Req. Poly No. $= M + 3$
1	2	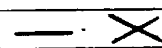	2*	4
1	3		3*	4
1	4		4	4
2	2		4*	5
2	3		6	5
3	2		6	6
4	2		8	7
* *singular matrix*				

Table 3. No. of Polynomials for Trim Using Mixed Method

Mixed Method					
M	N	β	p	No. of Poly $= 2M(N-1)$	Req. Poly No.
1	2	—	—	2*	6
1	3	/	/	4*	6
1	4	/ ∩	/ ∩	6	6
2	2			4*	6
2	3			8	6
3	2			6	6
* *singular matrix*					

Table 4. No. of Zeros and Polynomial Order of Displacement Formulation

N	Description	No. of Zeros including end points	No. of Zeros in intervals
2	Linear	2	0
3	Quadratic	3	1
4	Cubic	4	2
5	Quatric	5	3

Table 5. No. of Zeros and Polynomial Order of Mixed Formulation

N	Description	No. of Zeros including end points	No. of Zeros in intervals
2	Constant	0	0
3	Linear	1	1
4	Quadratic	2	2
5	Cubic	3	3
6	Quatric	4	4

REFERENCE

1. Riff, R. and Baruch, M., "Stability of Time Finite Elements', *AIAA Journal*, Vol. 22, No. 8, August 1984, pp1171-1173.

2. Baruch, M. and Riff, R., "Time Finite Element Discretization of Hamilton's Law of Varying Action", *AIAA Journal*, Vol. 22, No. 9, September 1984, pp.1310-1318.

3. Peters, David A. and Hohenemser, Kurt H.,"Application of the Floquet Transition Matrix to Problems of Lifting Rotor Stability," *J. American Helicopter Society*, Vol. 16, No. 2, April 1971, pp.25-33.

4. Borri, M., Lanz, M. and Mantegazza, P.,"Helicopter Rotor Dynamics by Finite Element Time Discretization," L'Aerotecnica Missilie Spanzio, Vol. 60, 1981, pp.193-200.

5. Borri, M., Mello, F., Iura, M. and Atluri, S. N., "Primal and Mixed Forms of Hamilton's Principle for Constrained and Flexible Dynamical Systems: Numerical Studies," ARO/AFOSR Workshop on Nonlinear Dynamics, Virginia Polytechnic Institute and State University, Blacksburg, Virginia, June 1988.

6. Ormiston, R. A. and Hodges, D. H., "Linear Flap-Lag Dynamics of Hingeless Helicopter Rotor Blades in Hover," *Journal of the American Helicopter Society*, Vol. 17, No. 2, April 1972, pp.2-14.

7. Peters, D. A., "Flap-Lag Stability of Helicopter Rotor Blades in Forward Flight," *Journal of American Helicopter Society*, Vol. 30, No. 41, October 1975, pp.2-13.

8. Hodges, D. H. and Ormiston, R. A., "Nonlinear Equations for Bending of Rotating Beams with Application to Linear Flap-Lag Stability of Hingeless Rotors," NASA TM X-2770, May 1973.

9. Hodges, D. H. and Hou, Lin-Jun, "Shape Functions for Mixed *p*- Version Finite Elements in the Time Domain," Presented at the Proceedings of SECTAM XV Conference, Atlanta, GA, March, 1990. Also to be appeared on *Journal of Sound and Vibration*, Vol. 144, No. 2, 1991.

10. Peters, D. A., "An Approximate Closed Form Solution for Lead-Lag Damping of Rotor Blades in Hover," NASA TM-62, 425, April 1975.

11. Wei, F. S. and Peters, D. A., "Lag Damping in Autorotation by a Perturbation Method," Presented at the 34th Annual National Forum of the American Helicopter Society, Washington, D.C., May 1978.

12. Peters, D. A. and Daniel P. Schrage, "Effect of Structural Parameters on the Flap-Lag Response of a Rotor Blade in Forward Flight," Interim Technical Report No. 1, U.S. Army Research Office, Grant No: DAAG29-77-G-0103.

13. Peters, D. A. and Izadpanah, A. P., "*hp*-version Finite Elements for the Space-Time Domain," *Computational Mechanics*, Vol. 3, 1988, pp.73-88.

14. Hodges, Dewey H. and Bless, Robert R., "A Weak Hamiltonian Finite Element Method for Optimal Control Problems," *Journal of Guidance, and Dynamics* submitted for publication.

15. Hodges, Dewey H., "Orthogonal Polynomials as Variable-Order Finite

Element Shape Functions," *AIAA Journal*, Vol. 21, No. 5, 1983, pp.796-797.

16. Babuska, I. and Szabo, B., Finite Element Analysis, Book Manuscript.

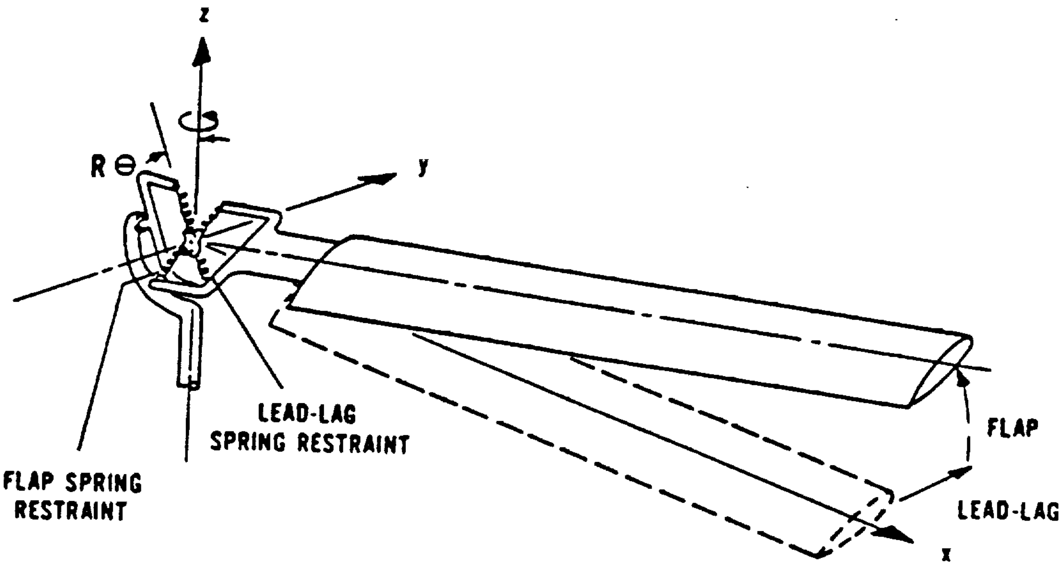

Fig. 1 Centrally hinged, spring restrained, rigid blade representation.

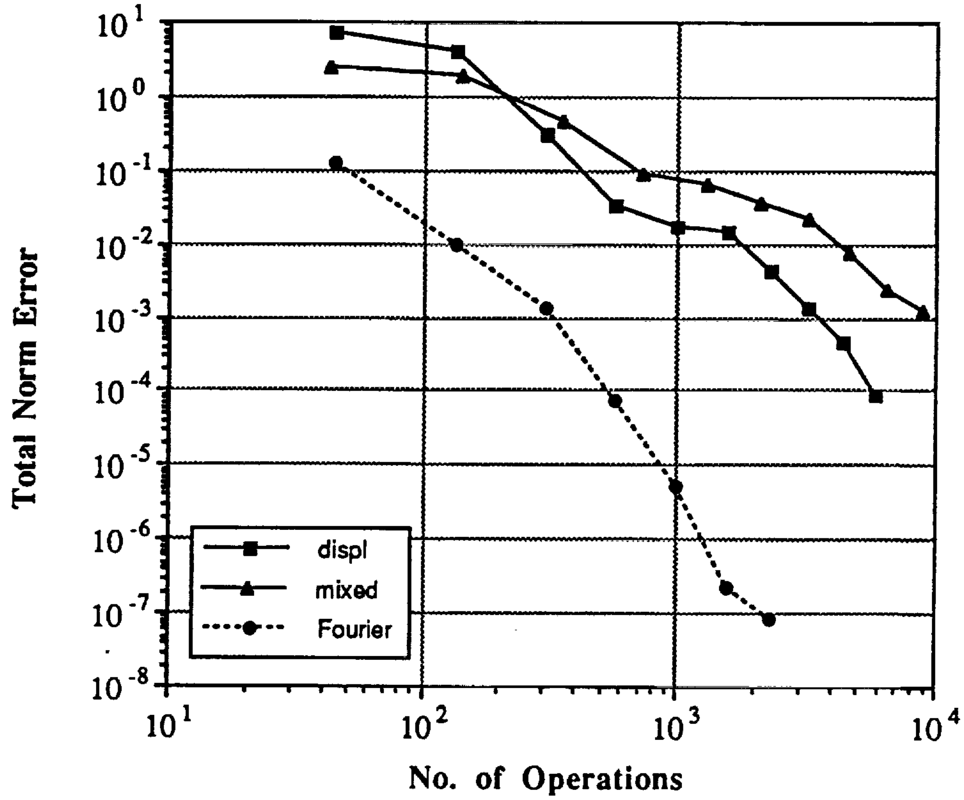

Fig. 2 Norm error vs. No. of operations for flapping (quasi-trim) with one element model.

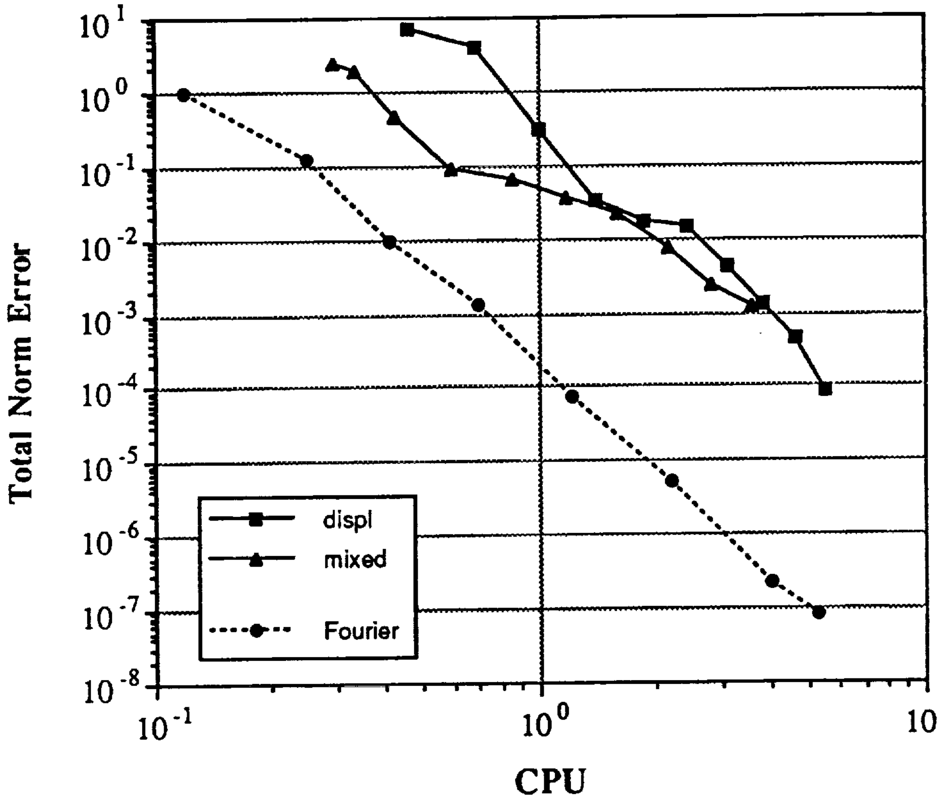

Fig. 3 Norm error vs. CPU for flapping (quasi-trim) with one element model.

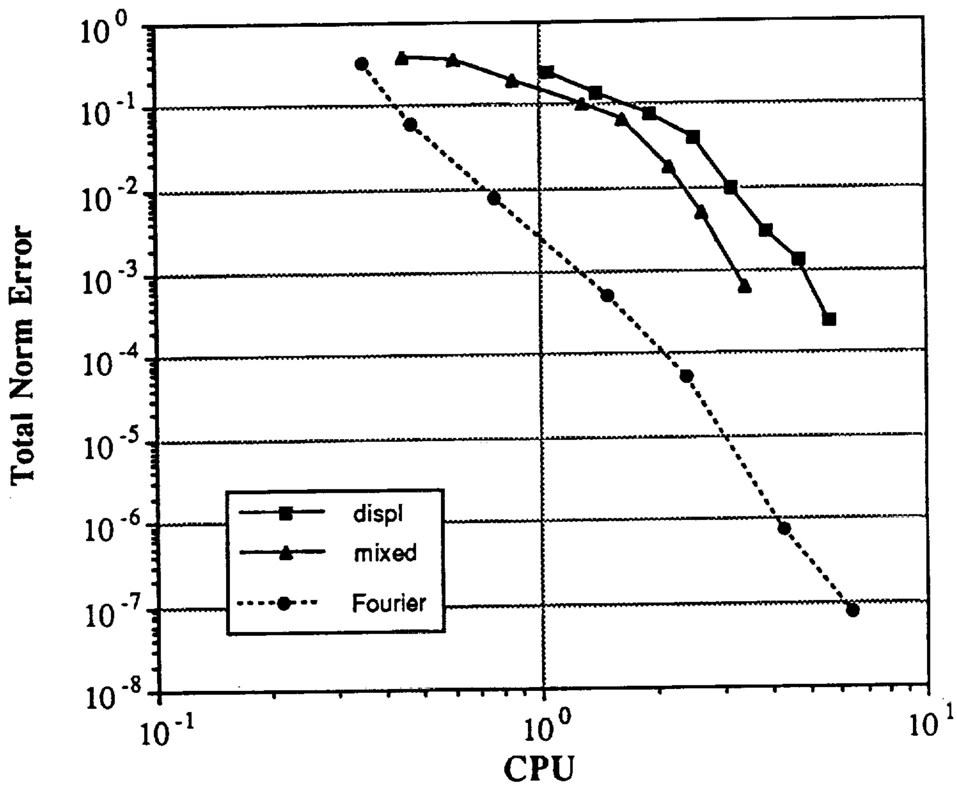

Fig. 4 Norm error vs. CPU for flapping (trim) with one element model.

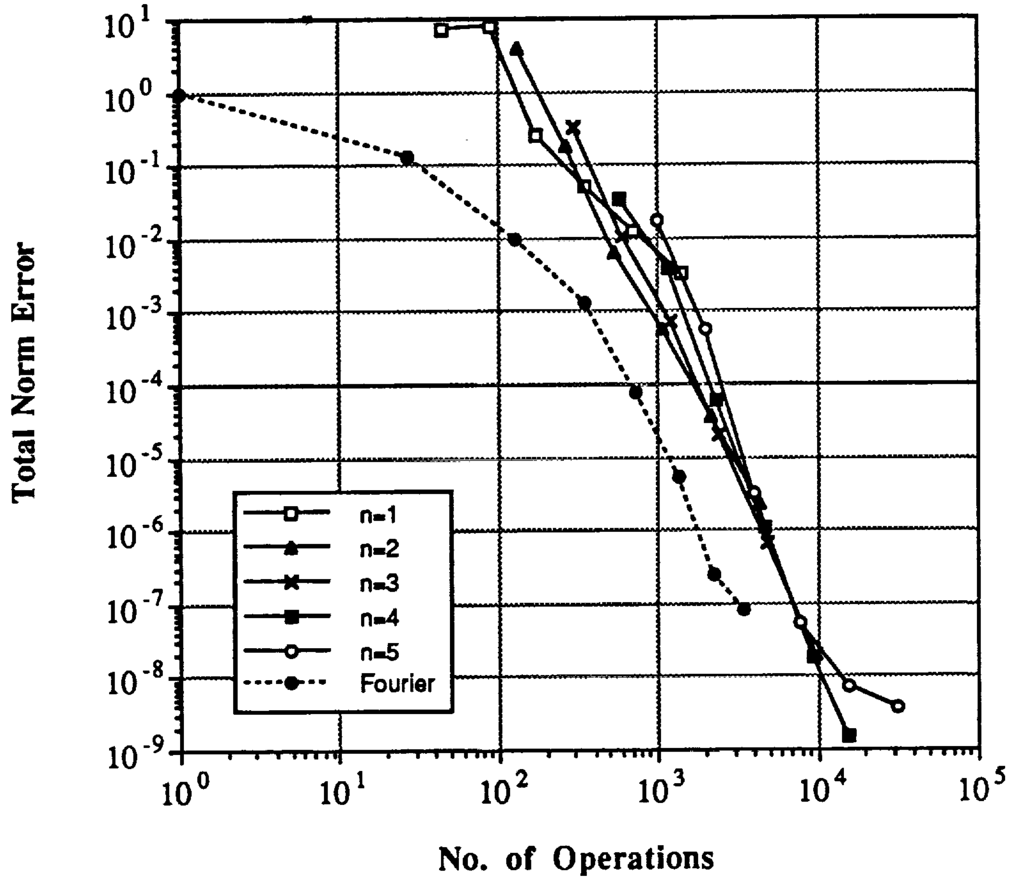

Fig. 5 Norm error vs. floating-point operations for flapping (quasi-trim) by displacement method compared with Fourier approach.

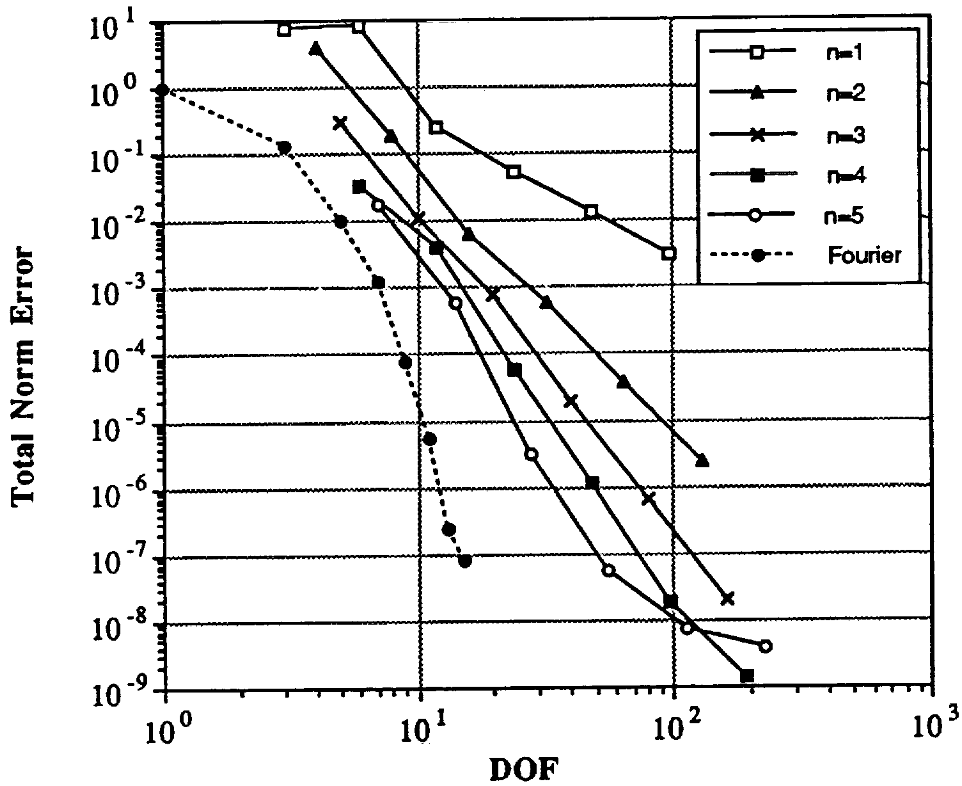

Fig. 6 Norm error vs. degrees of freedom for flapping (quasi-trim) by displacement method compared with Fourier approach.

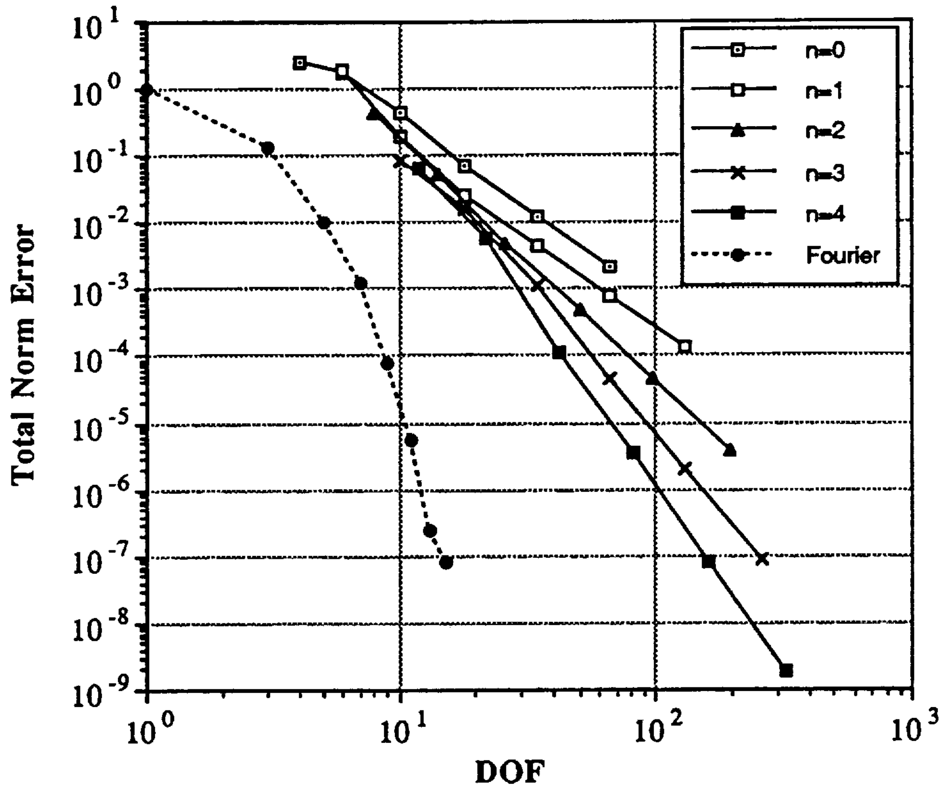

Fig. 7 Norm error vs. degrees of freedom for flapping (quasi-trim) by mixed method compared with Fourier approach.

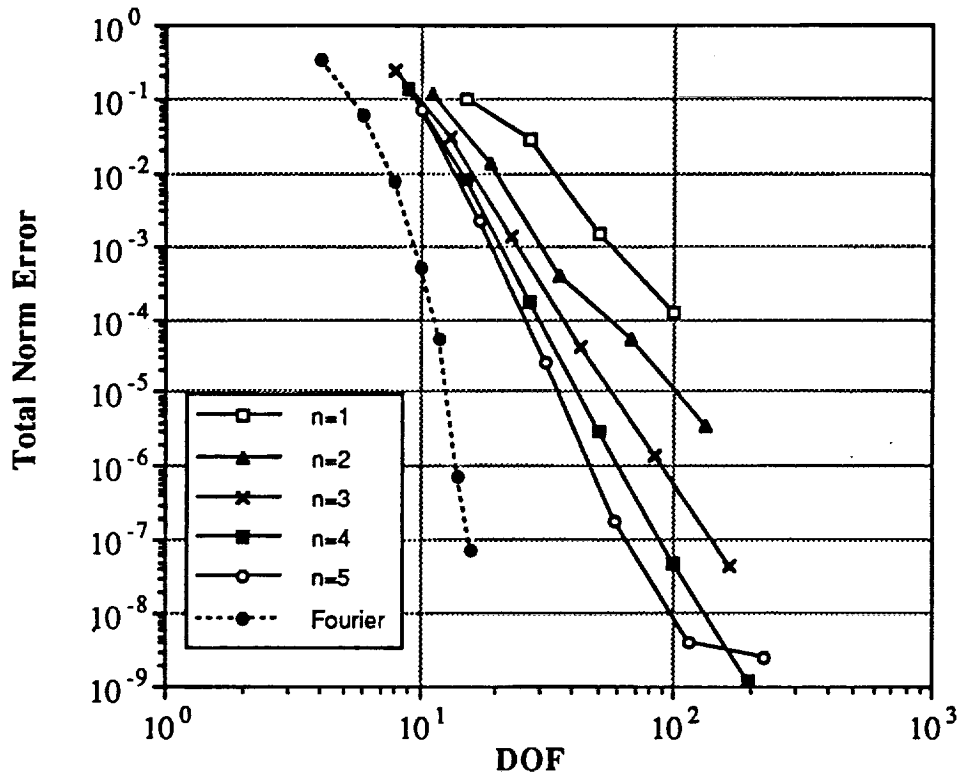

Fig. 8 Norm error vs. degrees of freedom for flapping (trim) by displacement method compared with Fourier approach.

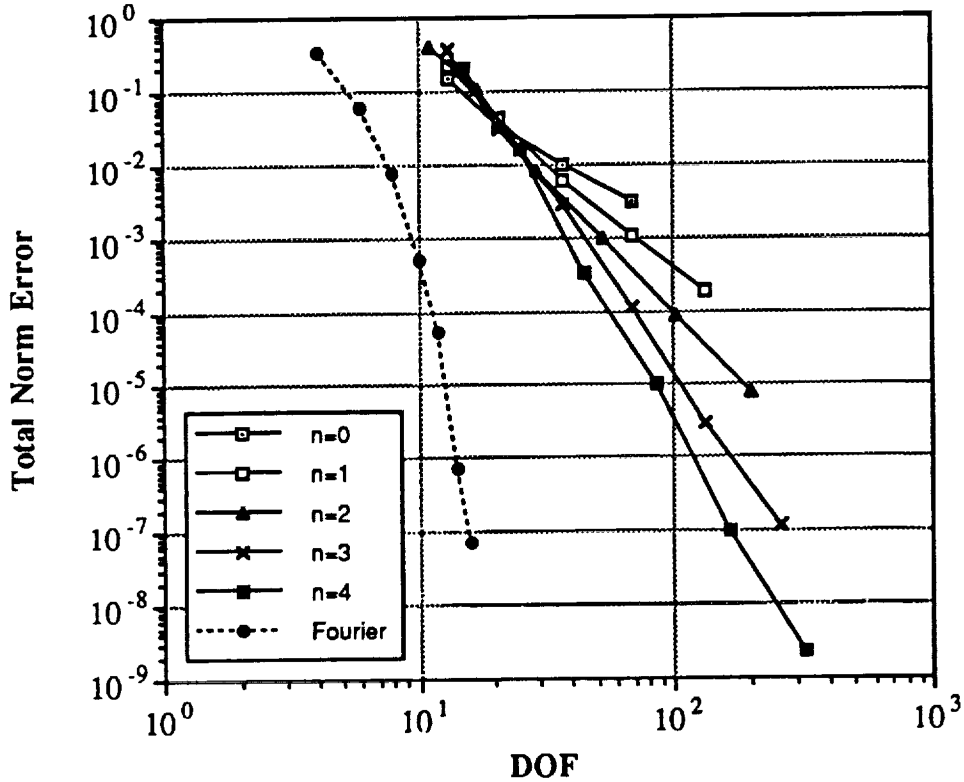

Fig. 9 Norm error vs. degrees of freedom for flapping (trim) by mixed method compared with Fourier approach.

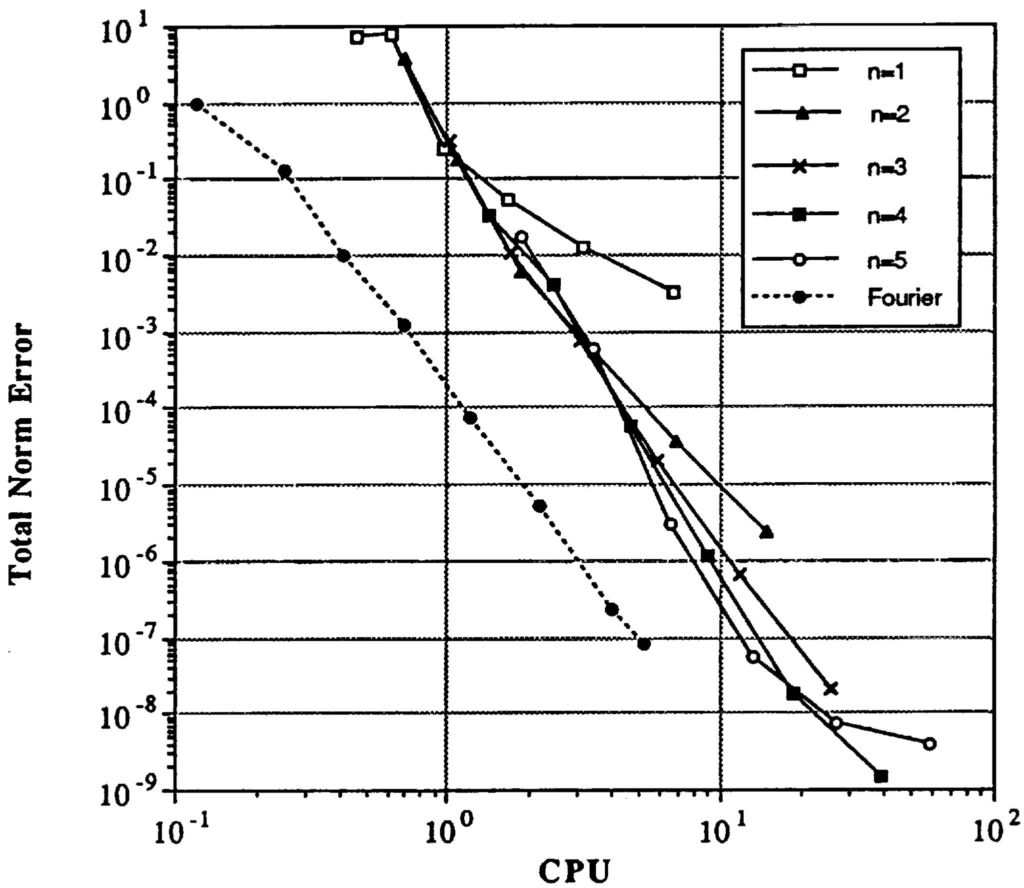

Fig. 10 Norm error vs. CPU for flapping (quasi-trim) by displacement method compared with Fourier approach.

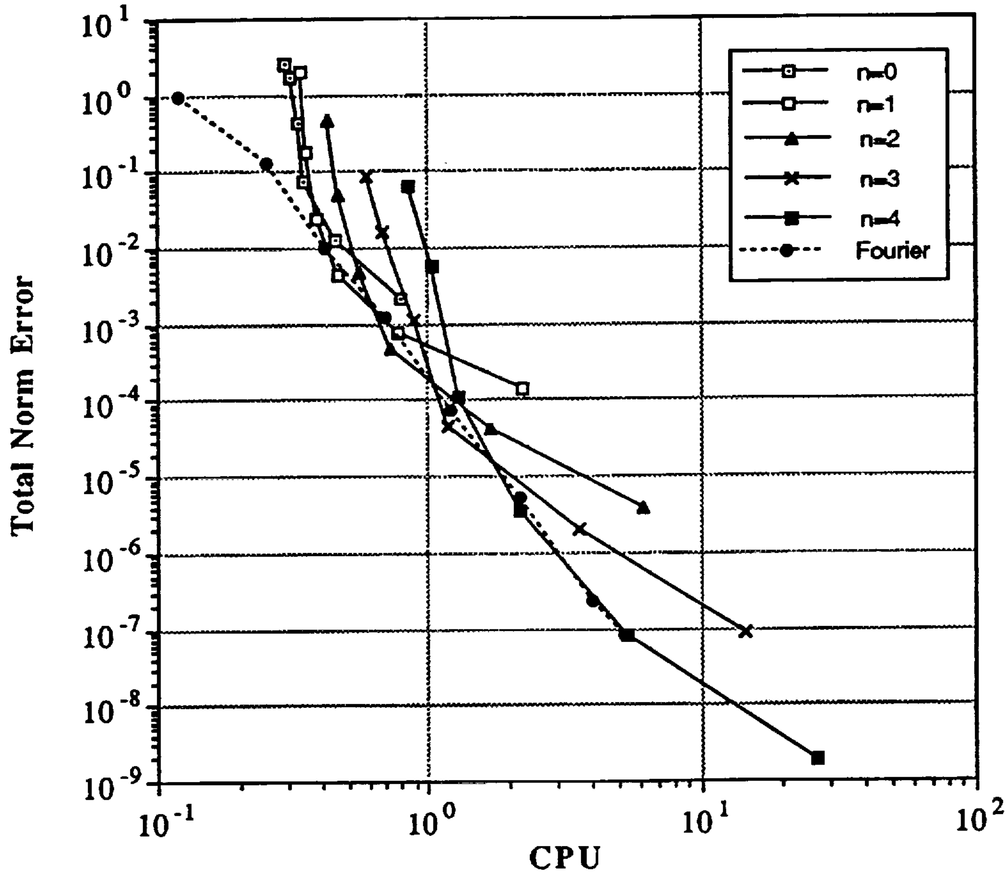

Fig. 11 Norm error vs. CPU for flapping (quasi-trim) by mixed method cpmpared with Fourier approach.

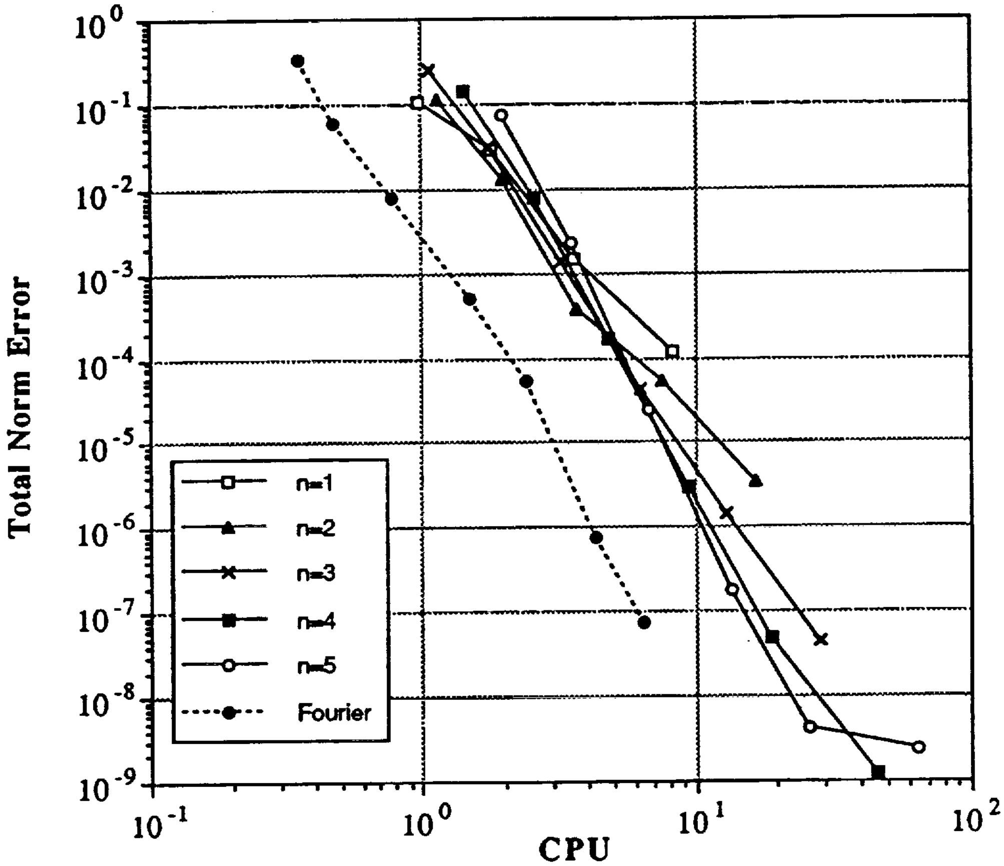

Fig. 12 Norm error vs. CPU for flapping (trim) by displacement method compared with Fourier approach.

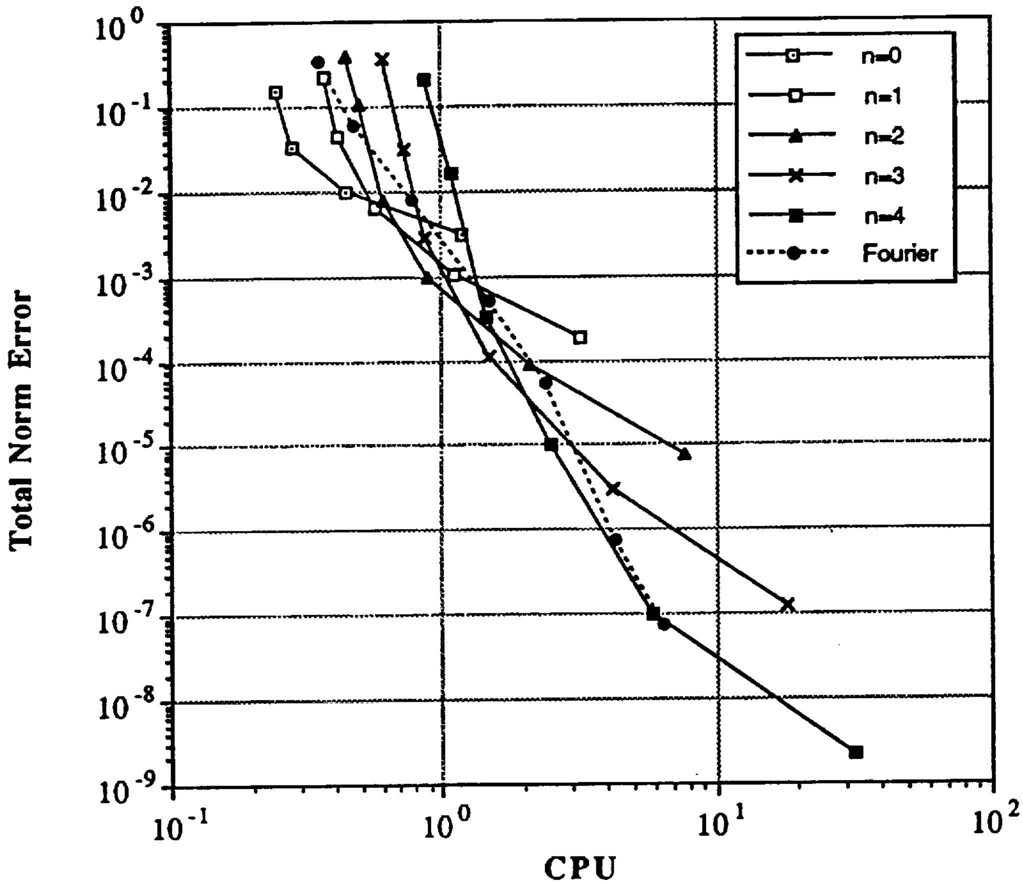

Fig. 13 Norm error vs. CPU for flapping (trim) by mixed method compared with Fourier approach.

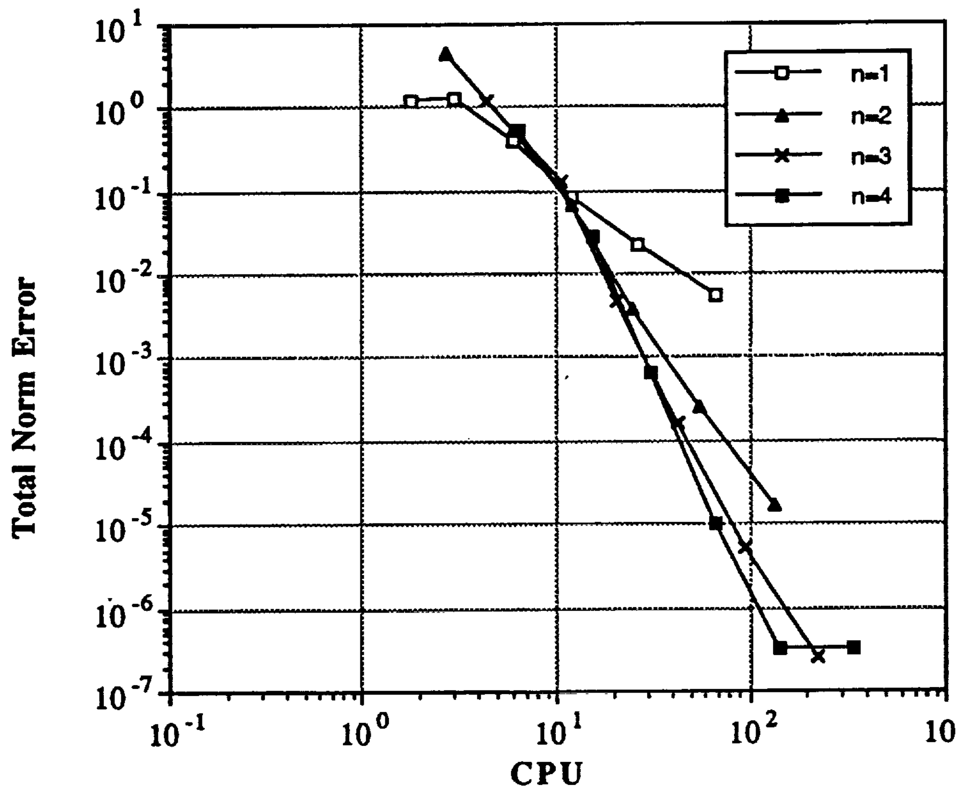

Fig. 14 Norm error vs. CPU for flap-lag (quasi-trim) by displacement method.

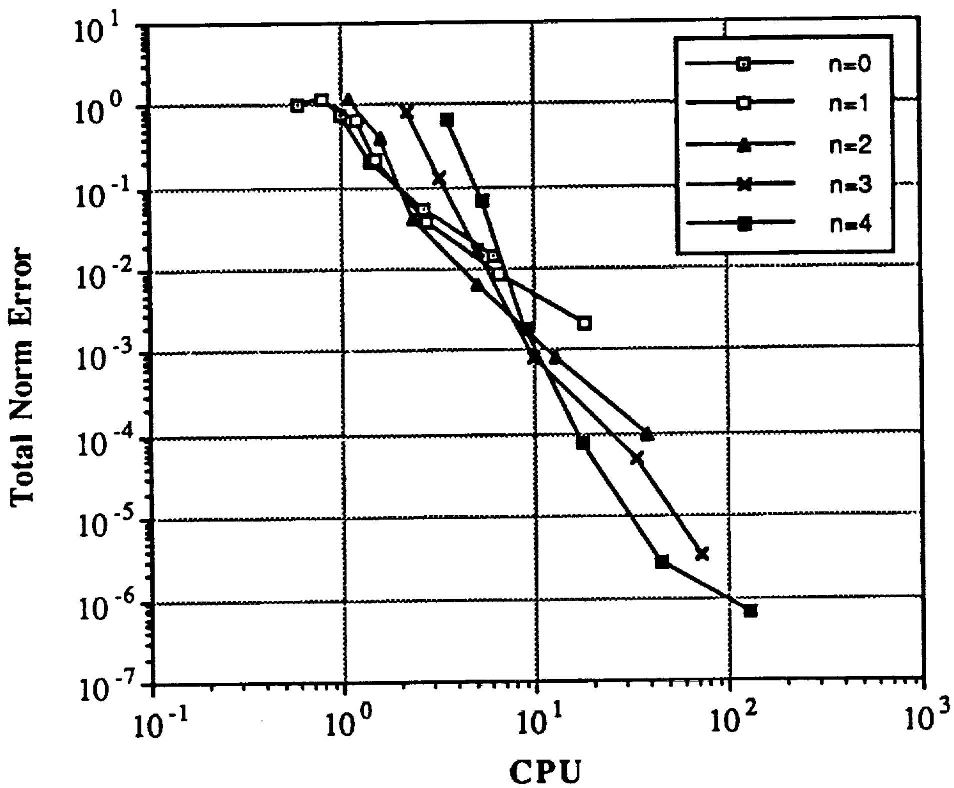

Fig. 15 Norm error vs. CPU for flap-lag (quasi-trim) by mixed method.

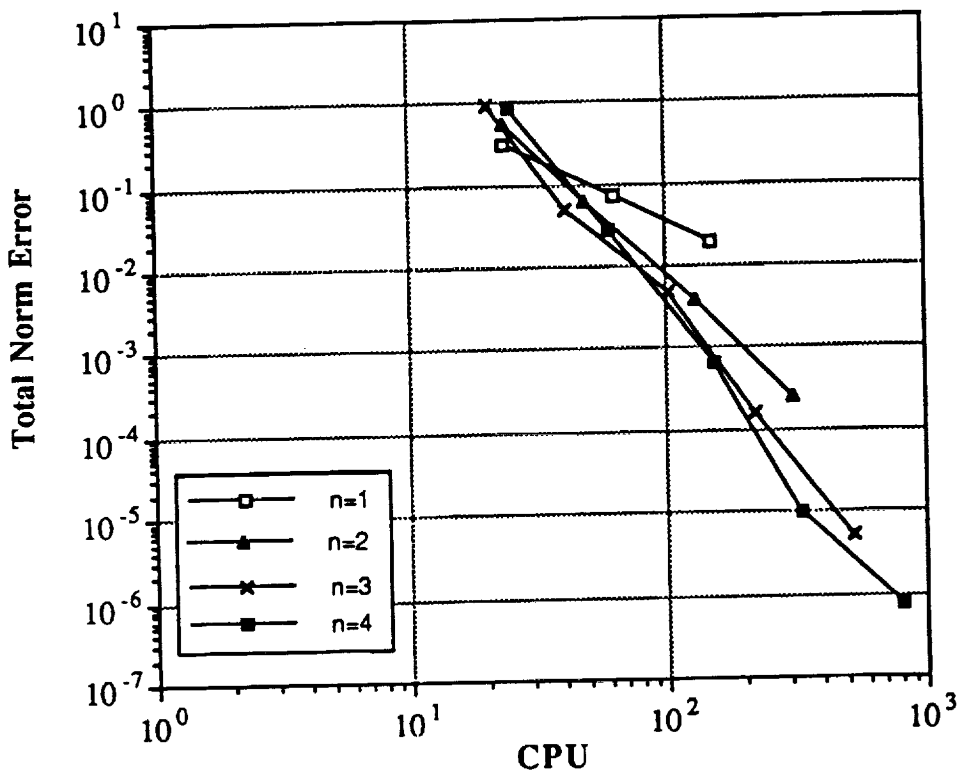

Fig 16. Norm error vs. CPU for flap-lag (trim) by displacement method.

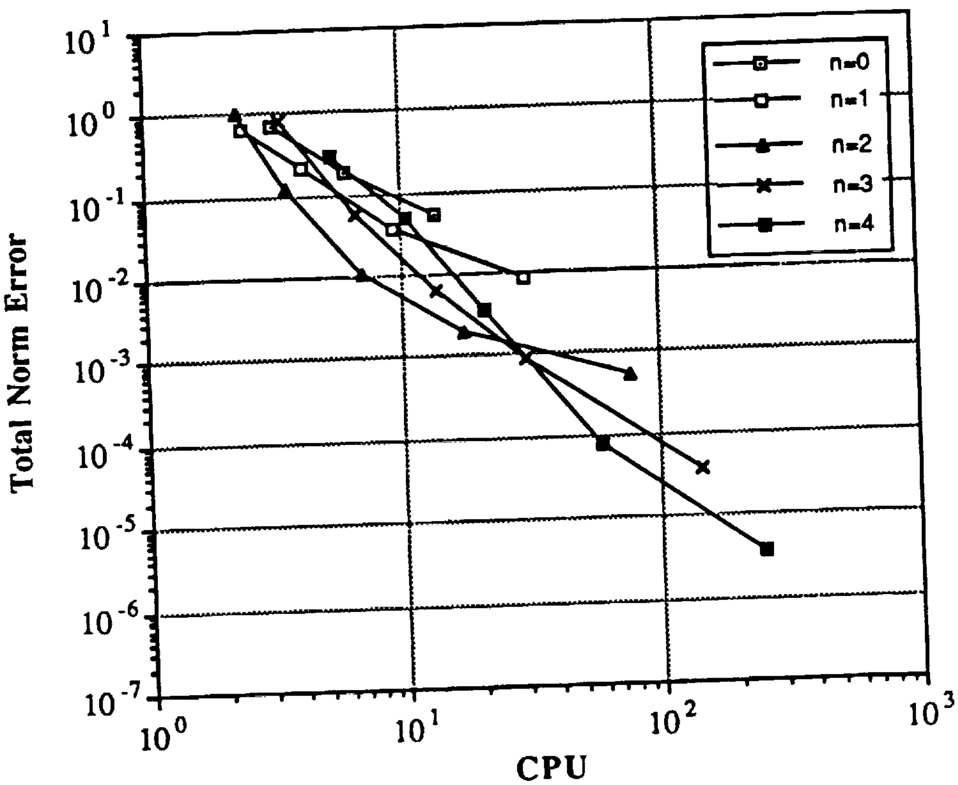

Fig. 17 Norm error vs. CPU for flap-lag (trim) by mixed method.